Mesoscale Weather Prediction with the RUC Hybrid Isentropic-Sigma Coordinate Model and Data Assimilation System

Stan Benjamin[1*], Rainer Bleck[2], John Brown[1], Kevin Brundage[1], Dezso Devenyi[1], Georg Grell[1], Dongsoo Kim[1], Geoff Manikin[3], Tom Schlatter[1], Barry Schwartz[1], Tanya Smirnova[1], Tracy Smith[1], and Steve Weygandt[1]

[1]*NOAA Research/Forecast Systems Laboratory, Boulder, CO*
[2]*Los Alamos National Laboratory, Los Alamos, NM*
[3]*NCEP/Environmental Modeling Center, Camp Springs, MD*

A paper presented at the Symposium on the 50th Anniversary of Operational Numerical Weather Prediction, 14-17 June 2004, College Park, MD

Note: Much of the material in this paper is taken from two recently published papers:

Benjamin, S.G., G.A. Grell, J.M. Brown, T.G. Smirnova,, and R. Bleck, 2004a: Mesoscale weather prediction with the RUC hybrid isentropic-terrain-following coordinate model. *Monthly Weather Review*, **132**, 473-494.

Benjamin, S.G., D. Devenyi, S.S. Weygandt, K.J. Brundage, J.M. Brown, G.A. Grell, D. Kim, B.E. Schwartz, T.G. Smirnova, T.L. Smith, and G.S. Manikin, 2004b: An hourly assimilation-forecast cycle: The RUC. *Monthly Weather Review*, **132**, 495-518.

Much of the material relating to the development history of the Rapid Update Cycle is new.

Paper presented at the Symposium on the 50th Anniversary of Operational Numerical Weather Prediction, 14-17 June 2004, College Park, MD

Mesoscale Weather Prediction with the RUC Hybrid Isentropic-Sigma Coordinate Model and Data Assimilation System

Stan Benjamin[1*], Rainer Bleck[2], John Brown[1], Kevin Brundage[1], Dezso Devenyi[1], Georg Grell[1], Dongsoo Kim[1], Geoff Manikin[3], Tom Schlatter[1], Barry Schwartz[1], Tanya Smirnova[1], Tracy Smith[1], and Steve Weygandt[1]

[1]*NOAA Research/Forecast Systems Laboratory, Boulder, CO*
[2]*Los Alamos National Laboratory, Los Alamos, NM*
[3]*NCEP/Environmental Modeling Center, Camp Springs, MD*

Abstract

The NOAA Rapid Update Cycle (RUC) is a mesoscale atmospheric data analysis and prediction system configured with a hybrid isentropic-sigma vertical coordinate and run operationally at the National Centers for Environmental Prediction (NCEP). The RUC model is the only quasi-isentropic forecast model running operationally in the world. Primary users include the aviation, severe weather, and general forecast communities, including National Weather Service Forecast Offices. The RUC is distinguished from other hybrid isentropic forecast systems by its application at a fairly high horizontal resolution (10-20 km), utilization of a high-frequency (hourly) analysis update cycle, and use of a continuous vertical coordinate formulation that allows purely isentropic model levels to extend into the lower troposphere.

The 2003 operational version of the RUC model and data assimilation system is described herein, complete with a discussion of the analysis formulation and model numerics and physical parameterizations. Within the 3DVAR analysis, use of the quasi-isentropic coordinate system for the analysis increments allows the influence of observations to be adaptively shaped by the potential temperature structure around the observation. Within the model, use of the hybrid $\theta-\sigma$ coordinate reduces the cross-coordinate vertical transport compared to a pure σ coordinate system. Examination of a 36-h forecast East Coast cyclogenesis case illustrates the detailed yet coherent nature of the potential vorticity, moisture, and vertical velocity structures produced by the quasi-isentropic RUC model.

---

[*] Corresponding author address
Stanley G. Benjamin
NOAA/Forecast Systems laboratory
325 Broadway, Boulder, CO 80305
(303) 497-6387
Stan.Benjamin@noaa.gov

1. Introduction

Many hazardous weather events are difficult to forecast even with very short lead-time. Specific examples include winter precipitation, convective storms, clear air turbulence, icing, and low ceiling and visibility. Accurate short-term forecasts of these phenomena are clearly important for the protection of life and property and also have significant economic value. Potential applications include aviation (air traffic management, flight routing and estimated fuel needs), agriculture, recreation and power generation.

In the early 1980s, scientists at both the National Meteorological Center (NMC, now NCEP) and the Program for Regional Observing and Forecasting Services, [PROFS, the dominant parent of the present Forecast Systems Laboratory (FSL)], realized that a new era was coming. With the advent of radiometric soundings available 24 hours per day from geostationary satellites (GOES), the prospect of frequent automated wind and temperature observations from commercial aircraft, and the developing technology of radar wind profiling promising high quality winds at hourly or more frequent intervals, it was clear that operational NWP could improve its product by capitalizing on this new supply of round-the-clock upper-air information. This led to an agreement on 6 April 1984 between NMC and PROFS, abetted by a Ron McPherson sabbatical at FSL, for FSL to take the lead in developing an assimilation/forecast engine that would ingest all available data at frequent intervals and combine them in some way with an NWP short-term forecast to produce a new analysis, and initialize a new forecast.

The expectation was that with this updated information, this later forecast would be superior to earlier forecasts, valid at the same time but initialized at the traditional 0000 or 1200 UTC, and that these forecasts would provide, perhaps for the first time, useful guidance for forecasting short-lived mesoscale weather phenomena. In fact, over the past 15-20 years, many different types of observations, some not foreseen 20 years ago, have become available over the United States (and globally), with frequencies of an hour or less. These include reports from commercial aircraft, radar wind profiles, images and radiometric soundings from geostationary satellites, reflectivity and radial velocity from scanning Doppler radars, estimates of column water vapor from ground-based GPS receivers, and automated surface reports.

This dream was realized when the first operational implementation of the Rapid Update Cycle (RUC1) occurred in 1994 (Benjamin et al. 1994), with a 3-h assimilation cycle (Benjamin et al. 1991) in which a new analysis was produced every 3 h using the previous 3-h forecast as a background. Major upgrades (Table 1) were made in horizontal and vertical resolution in 1998 (RUC2) and 2002 (RUC20). The 2002 version (hereafter RUC) employs 20-km horizontal resolution, 50 vertical levels, and a 1-h assimilation cycle. The RUC thus runs at the highest frequency of any forecast model at NCEP, assimilating recent observations to provide hourly updates of current conditions (analyses) and short-range numerical forecasts. The RUC is unique among operational numerical weather prediction (NWP) systems in two primary aspects: its hourly forward assimilation cycle, and its use of a hybrid isentropic/terrain-following vertical coordinate for both its assimilation and forecast model components.

2. Choice of isentropic coordinates

The use of entropy as a vertical coordinate has long had a strong conceptual appeal, since it was recognized that the entropy of dry air is monotonically increasing with height as viewed from a synoptic-scale perspective. This means that three-dimensional, adiabatic flows as viewed in ordinary Cartesian space can be represented as two-dimensional on surfaces of constant entropy, or, equivalently, potential temperature. The physical insights gained from this perspective have been foundational, dating back to the time of Rossby and earlier. In particular, the fundamental dynamical quantity, potential vorticity, has an especially simple scalar representation in the isentropic framework under the hydrostatic approximation:

$$(\zeta + f)\frac{\partial \theta}{\partial p} = const \qquad (1)$$

where ζ is the vertical component of relative vorticity and f is the vertical component of twice the earth's rotation vector. It then followed naturally, as the importance of numerical models to both weather forecasting and dynamical meteorology was recognized, that attempts would be made to formulate numerical models with potential temperature as the vertical coordinate.

Numerical atmospheric prediction using an isentropic vertical coordinate was first introduced in 1968 (Eliassen and Raustein), and for the last 35 years, isentropic modeling has received a modest yet steady stream of research attention. Much of this work has centered on recasting atmospheric representation using this coordinate to better handle the lower boundary condition, resulting in the development of a variety of hybrid isentropic/terrain-following coordinate models (e.g., Bleck 1978, Deaven 1976, Gall 1972, Uccellini et al. 1979, Johnson et al. 1993, Bleck and Benjamin 1993, and Konor and Arakawa 1997). As noted above, these efforts were all driven, at least in part, by a desire to translate the simplicity of the isentropic perspective of three-dimensional (3-D) baroclinic structures as shown by Rossby et al. (1937), Namias and others (see review by Gall and Shapiro 2000) into atmospheric modeling. While most applications of isentropic models up to this time have been in research, an exception is the RUC. The RUC model is also distinctive in its current application at a much finer horizontal resolution (currently 10-20 km) than previous isentropic models.

Apart from their dynamical appeal, isentropic-coordinate models are potentially advantageous in that they reduce (or eliminate, in the case of adiabatic flow) vertical transport through coordinate surfaces. In these models, lateral mixing is carried out on isentropic surfaces rather than across them, meaning that no unwanted cross-isentropic mixing occurs. Spurious growth of entropy in non-θ models, resulting in a cold bias in climate applications (Johnson 1997) or lack of ensemble spread (Egger 1999), is avoided. Weaver et al. (2000) show that laminar structures of ozone in polar regions are better represented with a 3-D off-line chemistry and transport model configured in isentropic coordinates than in a similar model using a sigma-pressure coordinate with more vertical levels. Diabatic effects from radiative flux divergence, always present in the atmosphere, and intermittent latent heating/cooling cause departures of material flow from isentropic surfaces. However, to a first-order approximation, isentropic surfaces are material surfaces in the free atmosphere.

Moreover, the moisture and potential vorticity environment for areas of precipitation may be forecast with better coherence using an isentropic model (Johnson et al. 1993, Bleck and Benjamin 1993). Isentropic coordinates are also advantageous in that they provide adaptive vertical resolution, greater in layers of higher static stability where strong vertical gradients of other variables are likely to occur. The concentration of isentropes in frontal zones of high thermal contrast means that these zones appear as larger-scale features in both along-front and cross-front dimensions when viewed in an isentropic perspective (e.g., Dutton 1976, Benjamin 1989, Gall and Shapiro 2000). All of these advantages of isentropic modeling in the atmosphere have counterparts in isopycnal modeling in the ocean (e.g., Bleck and Boudra 1981, Bleck 2002, Drijfhout 1992). This has led over the years to a two-way technology transfer that has benefited both fields.

In spite of these conceptual arguments for the use of isentropic coordinates, most of which were recognized at the time a rapidly cycling assimilation system was conceived, worldwide, no operational model was cast in any form of isentropic coordinate. How was it, then, that the RUC came to be so cast? The original intent, starting in 1983, was to design an initial prototype system based on an equivalent barotropic model (with help from Rainer Bleck) to establish a proof of concept. In the process of forming the group within FSL (called MAPS, for Mesoscale Analysis and Prediction System) that would build this system, there was hired a young Ph.D. from the University of Miami, a student of Rainer Bleck, who had been working with Mel Shapiro, then at the Wave Propagation Lab now Environmental Technology Lab, of NOAA on an Observation System Simulation Experiment to test the use of dynamical balance to extract temperature information from a hypothetical network of wind profilers. Renate Brümmer had thus been well infused with the advantages of isentropic coordinates, and she and Rainer Bleck were instrumental in convincing the other members of the group that a model based on them had viability. Furthermore, saddled with an older fleet of aircraft with inefficient, pre-turbofan engines and very high fuel prices as a recent memory, the airlines were putting demands on the National Weather Service to provide more accurate very-short-range upper-level wind forecasts. These needs of the aviation community were most clearly articulated by the FAA-sponsored Aviation Weather Forecasting Task Force of the mid 1980s. Because cruise altitudes are near the tropopause and jet stream, where there are generally strong variations in static stability, and because diabatic effects at these altitudes are generally small, the use of isentropic coordinates seemed a natural choice for a model serving the rapid-update function. An atmospheric analysis also configured in isentropic coordinates to complement an isentropic for an assimilation cycle had been developed by the late 1980s (Benjamin 1989).

The RUC numerical forecast model is an advanced version of the hydrostatic primitive equation model described by Bleck and Benjamin (1993 – BB-93). Its vertical coordinate is also used in the RUC assimilation system. The use of a generalized vertical coordinate in a numerical weather prediction model introduced in BB-93 is demonstrated again in this paper, but now in an application with much higher horizontal resolution (10-20 km compared to 100-160 km in BB-93) and increased emphasis on modeling of diabatic processes.

Here we emphasize issues in the design of hybrid isentropic models and describe experiments with the RUC model to investigate the particular issue of cross-coordinate vertical transport.

3. Design of hybrid isentropic-sigma models

Various hybrid-isentropic model schemes have been developed with the goal of retaining the advantages of isentropic representation while eliminating the main shortcoming of a pure isentropic scheme, which lies in the treatment of the planetary boundary layer or other layers where entropy is constant or even may decrease with height. While other hybrid coordinate models exist, especially hybrid sigma-pressure models with terrain-following coordinates (Phillips 1957) gradually turning into isobaric coordinates above some intermediate constant-pressure level, we limit our discussion here specifically to isentropic-sigma (θ-σ) hybrid coordinate definitions.

Bleck (1978) describes four different types of hybrid θ-σ models. All of these designs define a specific coordinate surface where σ representation near the ground makes a transition to θ representation aloft. One of these options (B), with the transition level at a fixed pressure distance above the surface, is found in the University of Wisconsin (UW) hybrid θ-σ model (Johnson et al. 1993). This model has been the basis for a number of studies that have demonstrated various numerical advantages of the hybrid coordinate representation over the pure σ representation (e.g., Johnson et al. 1993, Zapotocny et al. 1994, Johnson et al. 2000). Only one of the hybrid design options (option D) described by Bleck (1978) avoids coordinate intersections at the interface between θ and σ domains. In option D, an above-ground isentrope is specified as the lower boundary of the θ domain, with the atmosphere below that interface resolved by σ coordinates. An example of an option-D hybrid model is the global circulation model described by Zhu et al. (1992) which used a lowest pure isentropic level of 352 K, a value necessitated by the fact that observed surface potential temperatures over the Himalayas in summer reach as high as 335 K. Johnson and Yuan (1998) have developed an option-D variant of the UW hybrid global model (called a θ-η model) with a lowest pure isentropic level of 336 K.

Two other hybrid θ-σ designs have emerged since the Bleck-1978 hybrid design classification, neither of which use fixed transition levels. The first (which we label as option E) is the two-condition definition described by BB-93, which provides isentropic representation far closer to the ground than previous hybrid coordinate definitions. As described in BB-93, this definition marked a significant departure from previous definitions, avoided any interface level and, in fact, used an equation set written for a fully generalized vertical coordinate. The BB-93 design, incorporated into the RUC model with the implementation of the 40-km RUC-2 (Table 1) in April 1998, is derived from a hybrid-isopycnic approach in the ocean model of Bleck and Boudra (1981), of which the HYCOM (hybrid community ocean model) ocean circulation model (Bleck 2002) is a modern descendant. Perhaps the best way to characterize the present hybrid scheme is to call it Arbitrary Lagrangian-Eulerian (ALE), a term originally coined by Hirt et al. (1974). Note however, that our scheme goes far beyond ALE in that it adds the element of "coordinate maintenance", i.e., the migration of coordinate surfaces toward a set of predefined target surfaces, in this case isentropes, wherever minimum thickness conditions allow.

A second, more recent hybrid θ-σ design (which we label option F) defines the vertical coordinate as a linear combination of σ (terrain-following) and θ, as described by Konor and Arakawa (1997). The Konor/Arakawa design, like option E (BB-93), has no coordinate intersections. Zhu and Schneider (1997) adopted a hybrid coordinate similar to that of Konor and Arakawa into a general circulation model and showed improvements over a σ_p version of the same model. Purser et al. (2002) have described developmental work on a hybrid-isentropic coordinate that is similar to option F but uses a constant pressure at the top, similar to the Zhu et al. (1992) option D model.

With the hybrid coordinate definition used in the RUC model (option E), coordinate surfaces more than 100-300 hPa above the surface tend to be purely isentropic. This characteristic is similar to the UW hybrid θ-σ model (option B) but not the Konor-Arakawa hybrid model (option F) nor the UW θ-η model (option D). Thus, the RUC coordinate combines the advantages of the UW θ-σ model (isentropic coverage down to midtropospheric levels) with those of the Zhu et al. and Konor-Arakawa models (no intersecting surfaces). In resolving much of the troposphere with isentropic levels, this coordinate is desirable for the weather forecasting application of the RUC model .

Initial efforts to use a quasi-isentropic coordinate in a nonhydrostatic framework have been introduced more recently by Skamarock (1998) and He (2002). These models also use generalized vertical coordinate frameworks in which the target coordinate, based on a smoothed isentropic/sigma structure, can change with time.

4. Reduction of vertical transport in hybrid isentropic-sigma models

Among the advantages of using a largely isentropic coordinate in an atmospheric model listed in Section 2, one of the most significant is the reduction in artificial numerical dispersion resulting from vertical motion across coordinate surfaces, especially oscillatory motion associated with internal gravity waves. This reduction occurs because, under adiabatic conditions, vertical advection is identically zero in grid-point space in an isentropic model since 3-D atmospheric motion is captured in two dimensions on quasi-material θ surfaces. In situations with latent heating associated with ascending saturated air, an isentropic model will have some cross-coordinate vertical advection, but this advection will be of non-oscillatory nature and will generally be smaller than in a quasi-horizontal model. The reduction of vertical dispersion in isentropic models leads to improved transport of moisture and other scalar quantities, as demonstrated in global models with horizontal resolution of well over 100 km (Johnson et al. 1993, 2000, 2002). In this paper, we investigate cross-coordinate vertical transport in a hybrid θ-σ model applied at a horizontal resolution of 20 km.

The reduction in vertical advection found in quasi-isentropic models can be illustrated in the context of an inviscid version of the hydrostatic continuity equation, which is written in generalized vertical coordinates as

$$\frac{\partial}{\partial t}\left(\frac{\Delta p}{\Delta s}\right)+\nabla_s \bullet\left(\mathbf{V}\frac{\Delta p}{\Delta s}\right)+\frac{\partial}{\partial s}\left(\dot{s}\,\frac{\Delta p}{\Delta s}\right)=0 \qquad (2)$$

where $\frac{\Delta p}{\Delta s}$ is the pressure thickness between two generalized vertical coordinate (s) levels and s is the vertical level index. In quasi-horizontal models, the first term of this equation is ~0, meaning that any nonzero horizontal mass flux divergence (term 2) will cause mass to be transferred between layers (term 3) to maintain specified pressures at each level. In a θ-coordinate model without diabatic effects, the last term (vertical advection) is zero, implying that layers expand and contract depending on mass flux divergence. In other words, isentropic models achieve a reduction of vertical advection by replacing the balance between terms 2 and 3, which is typical of sigma or pressure coordinate models, with a balance between terms 1 and 2.

The RUC model is applied operationally at much smaller grid lengths than the University of Wisconsin θ-σ global model used by Johnson and his colleagues. Hence, extrema of diabatic processes are much more pronounced than on a coarse scale. Significant weather events, which the operational RUC is designed to predict, are often characterized by strong diabatic effects. Therefore, it is of interest to examine the mesoscale behavior of cross-coordinate vertical transport and the ability to conserve θ_e for moist reversible processes.

A set of experiments was carried out with the RUC model to investigate these issues. Alternative versions of the model were developed, one with the hybrid θ-σ coordinate definition and one using a "fixed" σ coordinate definition.

In result, the cross-coordinate vertical transport was reduced with the hybrid θ-σ coordinate definition by 30-35% for a summer case and 50% for a winter case, averaged over all levels. This reduction was much larger in the θ domain, by approximately 85% in these cases, and by 98% in further experiments with no diabatic effects allowed. The second set of experiments, investigating moist reversibility processes in a mesoscale application, confirmed the results of previous global scale experiments by Johnson and his colleagues: that use of a quasi-isentropic vertical coordinate provides a significant improvement in numerical accuracy in simulating these processes. A full description of these experiments is provided in Benjamin et al. 2004a.

5. Vertical grid structure

The definition of the RUC model vertical structure follows that described by Bleck and Benjamin (1993, section 2e). The RUC hybrid coordinate has terrain-following layers near the surface with isentropic layers above, as shown in Fig. 1, a vertical cross section of RUC coordinate levels from an actual case. The 20-km RUC uses 50 vertical levels, with each one assigned a reference or "target" virtual potential temperature (θ_v) value (Table 2). The algorithm used to define vertical levels by BB-93 is applied separately in each grid column and at every model dynamical time step and consists of only about 20 lines of code. Operating on one coordinate level at a time (see Table 3), the algorithm uses two criteria: 1) move the coordinate surface to the pressure where the target θ_v value is found (the *isentropic* definition), and 2) maintain a minimum pressure spacing between coordinate surfaces starting upward from the surface (the *sigma* definition). If the pressure yielded by the isentropic criterion (1) is less than that from the sigma criterion (2), the gridpoint pressure is defined as isentropic, otherwise as terrain-following (sigma). A "cushion" function (BB-93) modifies the minimum spacing in the transition zone between σ and θ definitions to avoid discontinuities in slope between the σ and θ portions of a given coordinate surface. From this two-part criterion, a new pressure, p_{new}, is defined at each grid point in the column. The coordinate level vertical

velocity, $\dot{s}\frac{\partial p}{\partial s}$, can now be calculated as

$$\dot{s}\frac{\partial p}{\partial s} = \frac{(p_{new} - \hat{p})}{\Delta t} \qquad (3)$$

where Δt is the model dynamical time step and $\hat{p}$ is the pressure at the outset of the vertical regridding procedure described in the previous paragraph. The value of $\dot{s}\frac{\partial p}{\partial s}$ will be zero on all levels where θ_v at the beginning of the regridding step matches the target value. If it is not zero, a new value of θ_v is also determined, as explained in BB-93, in a manner that avoids geopotential perturbations in the grid column above.

The minimum pressure spacing in the RUC is applied only between the ground and 600 hPa and is set as 2.5, 5, 7.5, and 10 hPa in the lowest 4 layers near the surface and 15 hPa at layers above that, providing adequate resolution of the planetary boundary layer and mixing near the surface. These minimum pressure thicknesses are reduced over higher terrain to avoid "bulges" of σ layers protruding upward in these regions (illustrated in Fig. 2).

The maximum θ_v value in the RUC20 is 500 K; this surface is typically found at 45-60 hPa for the operational RUC domain with a latitude range of ~15-60° N. A characteristic of the RUC hybrid coordinate is that more σ levels "pile up" near the surface in warmer areas, while more of the vertical domain is defined using isentropic surfaces in colder areas. This behavior, which is beneficial as it tends to provide high near-surface vertical resolution for convective boundary layer modeling during the warm season, and year-round at low latitudes, is apparent in Fig. 1. The case shown here is from 2 April 2002, with the cross section extending from Mississippi (on the left) northward through Wisconsin (center point), across Lake Superior (slightly higher terrain on each side), and ending in western Ontario. A frontal zone is present in the middle of the cross section, where the RUC levels (mostly isentropic) between 700 and 300 hPa are strongly sloped. In the RUC20, the isentropic levels from 270-355 K are resolved with no more than 3 K spacing (Table 2).

The adaptive variability of the generalized hybrid θ-σ coordinate used in the RUC is further explored in Fig. 2 (a vertical cross section of RUC hybrid levels for a winter case) and Fig. 3. The cross section in Fig. 2 is west-east across the United States, passing south of San Francisco, through the eastern slopes of the Rocky Mountains in Colorado (where a mountain wave is evident between 300-600 hPa) and through southern Virginia on the East Coast. Again, as in Fig. 1, the typical higher resolution using the RUC coordinate near fronts and the tropopause is apparent, as is the piling up of terrain-following levels in warmer regions (over the Pacific Ocean at the left side of the figure). A classic cold dome is evident over the central U.S., with a lowered tropopause and frontal zones extending to the surface on both sides.

Alternative perspectives of this same cross section are shown in Fig. 3, with pressure (Fig. 3a) and virtual potential temperature (Fig. 3b), both as functions of generalized coordinate level (k). These perspectives may be compared with the more familiar presentation in Fig. 2 to obtain some insights into the RUC hybrid coordinate. For instance, the θ_v vs. k cross section (Fig. 3b) shows that well over half of the generalized grid points in this depiction are resolved as isentropic levels. The σ layer (where generalized vertical levels have been resolved as σ levels) is deepest (in k space) at this time over the Rocky Mountains due to the combination of a relatively warm air mass and the lower surface pressure together with the minimum pressure thickness constraint. The daytime boundary layer is represented in k space as nearly vertical isotherms of θ_v isopleths near the surface (Fig. 3b).

The pressure vs. k cross-section (Fig. 3a) depicts pressure thickness between k levels ($\Delta p/\Delta s$, where s is the generalized vertical coordinate using the level k), larger where isobars are closely packed. In the 'isentropic levels' where θ spacing is constant, the closeness of isobars is proportional to $\partial p/\partial\theta$. Closely packed isobars in these isentropic levels represent lower thermal stability, common in the upper troposphere, whereas more loosely spaced isobars represent 'thin' RUC layers with higher static stability. These stable layers are found in the stratosphere, and also at lower k levels, where the tropopause is lower in the main upper-level trough associated with the cold dome located to the east (right) of the center of the cross section.

To provide a seasonal contrast in the behavior of the RUC hybrid coordinate, pressure vs. k and θ_v vs. k cross sections are presented in Fig. 4 for a summer case (25 July 2001) for the same west-east line as in Fig. 3. In this summer case, a much higher percentage of the RUC hybrid levels are resolved as terrain-following levels, about 30 out of the 50 levels (Fig. 4b). The boundary-layer depth in k space extends up to about k=30 (θ_v = 320 K from Table 2) over Colorado, but only up to approximately k=10 over most of the cross section away from the Rocky Mountains.

6. The RUC Model

The dynamical equations and their finite-difference approximations that form the basis for the RUC model are given in Benjamin et al. (2004a) and BB93. In addition to the horizontal momentum equations, the hydrostatic equation, the equation for continuity of mass, and the first law of thermodynamics, there are budget equations with source and sink terms for the mixing ratios of water vapor and each of the five hydrometeor species (cloud and rain water, cloud ice, snow and graupel) in addition to the number concentration of cloud ice. There is no vertical staggering of variables; only the mass continuity is applied to the layer between adjacent hybrid-isentropic coordinate surfaces.

The RUC is a full-physics model, that is, it contains parameterizations or representations of the main physical processes that involve subgrid vertical transports or processes that are too complicated to be described explicitly. In the current version of the RUC20 these are as follows.

- Short-wave radiation: Dudhia (1989) broadband with attenuation by O_3 and attenuation/reflection by grid-scale clouds
- Long-wave radiation: Dudhia (1989) broadband including absorption and reemission by clouds
- Land surface and surface fluxes: Smirnova et al (1997, 2000a) including two-layer snow, 6-layer soil and cycling of snow cover and snow water equivalent as well as soil temperature and moisture
- Subgrid turbulent vertical mixing: Pan et al (1994) in surface layer, modified Burk-Thompson (1989, based on Mellor-Yamada level 2) above the surface (including upper levels)
- Convection: Grell-Devenyi (2002) ensemble-closure scheme
- Grid-scale microphysics: mixed-phase bulk microphysics scheme used in the MM5 model (Reisner et al 1998, Thompson et al 2004) with explicit forecast of mixing ratios of cloud water, rain, cloud ice, snow, graupel, and cloud-ice number concentration, as well as diagnosis of variable number concentration for rain and snow

These schemes are summarized in Benjamin et al. (2004a) and described in more detail in the cited references. In addition to the coupling between the schemes noted above, detrainment from parameterized convection is a source term for grid-scale cloud water or cloud ice (depending on temperature) that is processed by the grid-scale microphysics.

7. Data Assimilation in the RUC

The Rapid Update Cycle uses a forward intermittent assimilation cycle, as depicted in Fig. 5. Every hour, recent observations are assimilated using the previous 1-h RUC model forecast as a background to produce a new estimate of 3-D atmospheric fields. Specifically, the observation-minus-forecast residuals (*innovations*) are analyzed to produce an estimate of the 3-D multivariate *forecast error field*, also called the *analysis increment*. This analysis increment is added to the 1-h forecast background to produce the new analysis. The 1-h forecast contributes information from previous observations into the current analysis through the filter of the forecast model. The observation types used by the RUC are discussed in Section 8.

The design of the prototype RUC (known then as the Mesoscale Analysis and Prediction System, MAPS) 3-h assimilation cycle, based on a pure isentropic coordinate and 80-km horizontal resolution, was described by Benjamin et al. (1991). The first isentropic analysis including assimilation of aircraft observations and suitable for initialization of this system was described by Benjamin (1989). The first version of the RUC running at NCEP (from 1994 to 1998) also used a 3-h assimilation cycle, thus missing two-thirds of the hourly observations (a situation remedied in 1998, when the RUC went to a one-hour cycle). Both of these 3-h cycles were continuous, in the sense that RUC forecasts were always used as the background for the next analysis. This internal cycling of regional models has become more common since that time, with the NCEP's Eta Data Assimilation System (EDAS) changing to fully cycled atmospheric variables in 1998 (Rogers et al. 1999).

We note two key issues associated with high-frequency forward assimilation: control of noise in the very short-range (1-h) forecasts used as the background for subsequent analyses (necessary to prevent accumulation of noise and imbalances), and time window design for grouping observations assumed to be valid at the analysis time (effectively, a trade-off between spatial and temporal resolution provided by the observations). These are discussed in more detail in Benjamin et al. (2004b).

Until May 2003, the operational RUC analysis was based on optimum interpolation (OI). Since then, it has been based on three-dimensional variational (3DVAR) analysis. Both methods are described in the textbook by Daley (1991).

Wherever the coordinate surfaces follow the isentropes in the RUC domain, the background error spatial covariances in the 3DVAR analysis are defined in a quasi-isentropic space. Thus, the influence of observations in correcting a background is adaptive depending on the 3D thermal structure in the vicinity of the observations. The background error covariances for all variables are specified as separable in the vertical and horizontal directions:

$$C_{i,j}^{m.n} = C_h(r_{i,j})C_v(|\,\theta_m - \theta_n\,|) \tag{4}$$

where C_h and C_v are the horizontal and vertical covariances, r is the horizontal separation between points *i* and *j*, θ is virtual potential temperature (see similar equation in Riishojgaard 1998), and *m* and *n* reference the coordinate surfaces for points *i* and *j,* respectively. Additional discussion on the use of a quasi-isentropic coordinate for the RUC analysis is provided in Benjamin et al. (2004b).

8. Operational aspects of the 20-km version of the RUC

a) Model grid, surface topography, and land surface characteristics

In the NCEP operational version as of this writing (May 2004) the RUC horizontal domain covers the contiguous 48 United States and adjacent areas of Canada, Mexico, and the Pacific and Atlantic oceans with a 20-km grid (Fig. 6). A Lambert conformal projection with a 301 by 225 rectangular grid point mesh is used. The grid length is 20.317 km at 35°N. Due to the varying map-scale factor from the projection, the actual grid length in the 20-km RUC decreases to as small as 16 km at the northern boundary.

The surface elevation of the RUC is defined using a *slope envelope* topography (also shown in Fig. 6). The standard envelope topography is defined by adding the subgrid-scale terrain standard deviation (calculated from a 10-km terrain field) to the mean value over the grid box. By contrast, in the slope envelope topography, the terrain standard deviation is calculated with respect to a plane fit to the high-resolution topography within each grid box. This gives more accurate terrain values, especially in sloping areas at the edge of high-terrain regions. It also avoids a tendency of the standard envelope topography to project the edge of plateaus too far laterally onto low terrain regions.

In addition to topography, there are other surface fields required by the RUC, including land use (needed for surface roughness, albedo), vegetation fraction, soil type, rooting depth (all used by the land-surface scheme), and sea- and lake-surface temperature. Most of these fields are the same as used by the EDAS (Eta Data Assimilation System).

b) Sources of observations for the RUC

In order for a high-frequency assimilation cycle to result in improved short-range forecasts, adequate high-frequency observations must exist over the domain of the analysis and forecast model. Over the last 10 years, the volume of observational data over the United States has increased, along with the sophistication of techniques to assimilate those observations.

A summary of observational data available to the RUC as of spring 2003 is shown in Table 4. Many types of observations are assimilated, most being limited in horizontal or vertical spatial coverage. The longest-standing atmospheric observing systems, rawinsondes and surface weather observations, are the only ones that provide complete observations of wind, pressure, temperature, and moisture. High-frequency wind observations above the surface are available from commercial aircraft (e.g., Moninger et al. 2003), wind profilers, satellite-estimated cloud motion, and radars (velocity azimuth display, VAD). High-frequency temperature observations above the surface assimilated by the RUC include commercial aircraft and a few from RASS (Radio Acoustic Sounding System). High-frequency moisture observations above the surface used in the RUC analysis are precipitable water retrievals from satellites (GOES and polar orbiter) and from ground-based GPS (Wolfe and Gutman 2000, Gutman and Benjamin 2001), and GOES cloud-top pressure/temperature retrievals (Schreiner et al. 2001). The "cut-off" time for availability of observations is very short with the RUC, generally about 20 min after the analysis valid time.

We note that most of these observations not subject to time windowing are, strictly speaking, valid 15-30 min before their labeled time. For instance, rawinsondes are launched about 45 min before valid time, surface observations are taken 15 min before valid time, and wind profiler hourly observations are hourly means centered 30 min before valid time. Accordingly, the time window used in the RUC for aircraft and cloud-drift wind observations is a 1-h window centered 30 min before "valid" time. This 15-30 min offset between labeled and actual valid time is present not only in the RUC but in other operational systems initialized with the same observations.

c) Quality control of the observations

Observation quality control in the RUC is primarily based on a buddy check between neighboring observations. Before buddy check or other quality control procedures proceed, gross quality control tests (range limits, wind shear, lapse rate) are applied to all observations. The buddy check considers observation innovations, the differences between the observation and the background field interpolated to the observation point instead of the observations alone. This is an important distinction, since it means that any known anomaly in the previous forecast has already been subtracted out, improving the sensitivity of the QC procedure to actual errors. The RUC buddy check is based on an optimum interpolation method whereby an estimate at the observation point is made from the innovations of a group of up to 8 nearby “buddy” observations, similar to that described by Benjamin et al. (1991). If the difference between the estimated and observed innovations exceeds a predefined threshold, the observation is flagged. For each observation, the QC check is repeated removing one of the buddies at a time to increase the robustness of the check. Because the RUC utilizes a partially flow-dependent adaptive (quasi-isentropic) background error structure, its buddy check method has some adaptivity. Isolated observations where no buddies are available are flagged if their innovation exceeds a variable-dependent multiple of the background error.

Checks are also made for contamination of VAD and profiler wind observations due to bird migration. Prior to dissemination of the data, a careful check for bird (and other) contamination in profiler winds is made at the Profiler Hub in Boulder, CO. This check includes use of second-moment data to examine likelihood of bird contamination. If the quality control flag produced by this check indicates suspicious data, the profiler data at that level are not used. For VAD winds, no second-moment data are available, so a more conservative check is made. A solar angle is calculated, and if the sun is down and the temperature is higher than -2°C, VAD winds are not used if they have a northerly component between 15 August and 15 November or a southerly component between 15 February and 15 June.

d) Details on 3DVAR assimilation

The accuracy of an analysis is dependent on the effectiveness of algorithms used to match observations with the background values through calculation of observation-minus-background differences (or innovations). These calculations are performed by so-called *forward models* that generate the model’s best estimate of the observed value from the prognostic variables at hand. The forward calculation may include variable transformation and always includes spatial interpolation from the model grid to the observation locations. For near-surface observations, the forward model should also account for elevation differences between the background and observations using expected boundary-layer structure. For surface observations, this treatment in the RUC analysis uses surface-layer similarity to match 2-m temperature and moisture observations and 10-m winds to the RUC background whose lowest level is at 5 m above the surface. Surface observations including a station pressure (from an altimeter setting) and station elevation are reduced to a surface pressure at the model elevation, and then to a height innovation at the model surface pressure. Observations of pressure reduced to sea level are not used in the RUC, since altimeter setting is less ambiguous and more commonly available over North America. Rawinsonde profiles from mandatory and significant level data are further interpolated to each model level, yielding additional data points. This forces the analysis to fit the near-linear structures implied by the absence of intermediate significant levels. The processing of each observation type to provide the best match between the observation and background is discussed in detail by Devenyi and Benjamin (2003).

A summary of fields updated in the RUC analysis (see Benjamin et al. 2004b and Devenyi and Benjamin 2003 for more details) is presented in Table 5. Note that the upper level of soil or snow temperature is also updated from surface air temperature analysis increments to preserve the air-surface temperature difference from the background field. (In general, the regional evolution of soil temperature and moisture fields and snow water equivalent and snow pack temperature fields has been found to give satisfactory results in the RUC (Smirnova et al. 1997, 2000a)). These fields are strongly dependent on the accuracy of the series of 1-h forecasts produced by the RUC, and therefore, vulnerable to precipitation spinup (or spindown) problems.

Hydrometeor fields are also cycled and modified using the cloud analysis technique described in Benjamin et al. (2004a), contributing to this result. Current development efforts to add radar reflectivity to this hydrometeor analysis (Kim et al. 2002) should further improve the RUC 1-h precipitation forecasts.

Within the RUC analysis, all of the above procedures and actual solution of the analysis increment, where mapping of observations and background values to vertical levels is required, are carried out using the 3D pressure of the background field, without regard to the algorithm defining the vertical coordinate that resulted in the 3D pressure field. As a final processing step (which is specific to the hybrid coordinate used in the RUC model), a vertical regridding (interpolation) occurs for all variables that restores them to the RUC hybrid isentropic-sigma coordinate definition described in Benjamin et al. (2004a).

Postprocessing of native RUC analysis fields is then performed to diagnose many other variables, including height (via hydrostatic integration), special level variables (freezing, maximum wind, and tropopause), cloud top, ceiling, visibility, convection-related indices, potential wind gust, and boundary-layer height (Benjamin et al. 2002). Hourly time series of full output at selected stations are created as part of the RUC post-processing.

e) Lateral boundary conditions

For any limited area model, the skill is increasingly controlled by the lateral boundary conditions (LBC) over time as the duration of a forecast increases. The LBCs for the RUC model, both in operations at NCEP and runs at FSL, are relaxed (Davies and Turner 1977) toward the NCEP Eta model (Black 1994, currently initialized every 6 h), linearly interpolated between 3-h output times. For RUC forecasts initialized at 0000 or 1200 UTC, the Eta model run used for LBCs is always the one initialized 6 h earlier (e.g., the 0600 UTC Eta run is used to prescribe LBCs for the RUC run initialized at 1200 UTC). This choice is made to provide RUC guidance to users as soon as possible as opposed to running the RUC model after the current Eta run is available. From a forecast skill standpoint, a 24-h RUC forecast run in this real-time configuration is controlled, to some extent, by the skill of the 30-h Eta forecast. Similarly, 12-h RUC forecasts are driven toward the information of the 18-h Eta forecasts valid at the same time. RUC forecasts can also be run using LBCs from Eta model runs initialized at the same time to provide a model intercomparison, but that was not done for the results shown here. LBCs for the RUC can be prescribed from other models such as the NCEP Global Forecast System (GFS) model, but the Eta model has been used for the RUC in operational runs up to this point since it is available sooner and has a higher horizontal resolution than the GFS model.

9. Brief comments on performance

The RUC is effective in its goal of providing more accurate short-range forecasts initialized with recent data than longer-range forecasts verifying at the same time (Benjamin et al. 2004b). This is the goal, of course, of any assimilation cycle, even on a 12-h frequency, but the RUC is unique in that it runs on a 1-h cycle and is successful in providing improved forecasts down to this projection. For all variables and levels except heights at 850 and 700 hPa, the RUC 3-h and 1-h model forecasts are more accurate than corresponding 3-h and 1-h persistence forecasts, on the average, over a 4-month evaluation period.

Extensive verification shows that the ability of the RUC to use irregularly distributed high-frequency observations to provide improved forecasts aloft at increasingly shorter durations is most evident for wind and temperatures, where an increase in skill is shown down to a 1-h forecast at all mandatory levels. For heights, 6-h RUC forecasts show a strong improvement over 12-h forecasts valid at the same time, but 1-h and 3-h forecasts do not in the lower troposphere. For relative humidity forecasts, this ability for improved short-range forecasts is mixed, certainly in part due to an absence of *in situ* high-frequency moisture observations over the United States except at the surface. One-hour RUC forecasts have errors that are 15-30% lower than for 12-h forecasts in the layer from 850-200 hPa. For wind forecasts, the errors are 25-50% lower at one hour than at twelve hours in the same layer. Short-range RUC forecasts of 2-m temperature and dewpoint temperature and 10-m wind also show an increase in skill down to a 1-h forecast over longer-range forecasts valid at the same time. For both forecasts aloft and at the surface, the RUC short-range forecasts show a strong improvement over corresponding persistence forecasts at 3-h and even at 1-h projections, a difficult test for numerical forecast models at such a short range. The challenge for the RUC is to use irregularly spaced and usually sparse observations to extract a net improvement in forecast skill, which it is able to do. Verification of the RUC at 24 h shows modest growth of error from 12 h to 24 h and that 24-h RUC model forecast skill approaches that of a 3 h persistence forecast.

10. Case Study

In this section, we present a brief case study from Benjamin et al. (2004a) of a 36-h forecast using a 20-km version of the RUC model for a case of cyclogenesis (1200 UTC 4 February – 0000 UTC 6 February 2001) along the east coast of the United States. Initial conditions for this case are provided by the RUC analysis (Benjamin et al. 2004b). Lateral boundary conditions are prescribed from the operational Eta model initialized at 1200 UTC 4 February. We adopt a quasi-isentropic perspective for this case, using maps of the pressure of the dynamic tropopause (defined as the first pressure, starting from the top of each column of the native hybrid θ-σ grid, at which potential vorticity (PV) drops below 2.0 PV units) as an indicator of the overall upper-level dynamics. At the 12-h forecast (valid 0000 UTC 5 February), the tropopause pressure (Fig. 7a) shows a major wave with a slight positive tilt over the eastern U.S., with a base near the Arkansas-Louisiana border and embedded waves over Illinois and Michigan. These three features are traceable to the 24-h forecast of tropopause pressure (Fig. 7b), at which time the base of the wave is located over southern Alabama and the embedded waves are merging over the southern Appalachians. By 0000 UTC 6 February (36-h forecast, Fig. 7c), the tropopause pressure shows a pronounced negative tilt, with a classic hook of lowered tropopause now rotating north-northeastward over southern New England with a trailing wave off the North Carolina coast. The continuity of fine filamental features in the tropopause and PV in these forecasts is typical for the RUC model. In the corresponding sea-level pressure (SLP) field evolution (see Benjamin et al. 2004a), as the upper trough approached the coast, a classic secondary low developed off the Georgia coast and subsequently moved northeastward, crossing shore in the forecast slightly to the west of the actual track.

Vertical cross sections were taken along a north-south (with respect to the grid) line through central Connecticut from the 20-km RUC 36-h forecast of θ, potential vorticity, relative humidity, and vertical velocity (Fig. 8) to give an additional 3-D perspective on the lower- and upper-level trough at this time. The three lowered tropopause undulations apparent in Fig. 8a may be matched to areas of low tropopause pressure evident in Fig. 7c, with the central extrusion associated with the surface cyclone. A center of high PV, associated with latent heat release, is evident along the surface-based front. Areas of slight negative PV are shown over the ocean in the marine boundary layer where sensible heating is occurring, and over Quebec where the absolute vorticity is slightly negative. The main wave near southern New England is also associated with dry air subsiding to its south to nearly 900 hPa (the dry slot) and nearly saturated air along the front in a plume up to almost 400 hPa (Fig. 8b). This moist air is associated with upward vertical motion up to -80 $\mu b\ s^{-1}$ in the 36-h RUC forecast (Fig. 8c). This case is presented as a demonstration of interacting dynamical and precipitation processes in the RUC model for a case with strong development.

11. Final comments

The Rapid Update Cycle (RUC) model is a hybrid isentropic / terrain-following model suitable for mesoscale weather prediction, fully compatible with parameterizations of diabatic and/or subgrid-scale processes typically used in operational models of this resolution. Running operationally at 20-km resolution, the RUC model is the only hybrid θ-σ model used for operational prediction at this time.

One of the primary advantages of modeling in isentropic coordinates, reduced cross-coordinate vertical transport, has been demonstrated in real-data experiments.

It is relevant to discuss here our perception of the weaknesses of the RUC model as currently configured. These include inaccuracies in vertical cross-coordinate transport due to use of a nonstaggered vertical grid and the fairly common presence of a large value of

$\frac{\partial^2 p}{\partial s^2}$ (where p is pressure and s is coordinate level) at the interface of the theta and sigma domains despite application of the cushion function, especially when cross-coordinate vertical mixing and transport is large, such as when a daytime mixed layer extends above this interface. The nonstaggered vertical grid in the RUC model was initially adapted for compatibility with nonstaggered data assimilation. As discussed in BB-93, it does not fully conserve potential vorticity.

Despite these possible issues, the hybrid θ-σ RUC model has been shown here to reduce vertical dispersion caused by cross-coordinate vertical transport compared to quasi-horizontal models, and thereby to improve numerical accuracy for moist reversible processes. It produced an accurate forecast with sharply defined 3-D dynamical and moisture structures for a case study at 20-km resolution.

Plans for the next two years include introduction of improved cloud/hydrometeor analysis techniques including assimilation of radar assimilation and surface cloud and current weather observations, recalculation of forecast background error covariances, testing of a *diabatic* digital filter initialization (Huang and Lynch 1993) and revised techniques for assimilation of all surface observations. We will also focus on better use of radar and satellite-based observations, especially to improve short-range forecasts of precipitation. The RUC will also move to higher horizontal resolution, with a planned upgrade to 13-km resolution in 2005.

The Rapid Update Cycle will make a transition to a version based on the Weather Research and Forecast (WRF) model and assimilation system (e.g., Skamarock et al. 2001) over the next several years. The techniques found to be essential for effective high-frequency assimilation in the current Rapid Update Cycle will be incorporated, as necessary, into WRF-based versions of future operational rapid updating assimilation and forecast systems that will be descendants of the current RUC.

Acknowledgments. The development of the RUC has been supported by the FAA Aviation Weather Research Program, NOAA Office of Global Programs, and NOAA Research, including the High Performance Computing Initiative. We thank many colleagues who have assisted us in the development, testing, and implementation of versions of the RUC, including colleagues at FSL, in particular, Steve Koch, at NCEP/EMC (Drs. Geoff DiMego, Eric Rogers, Dave Parrish, Jim Purser and Wan-Shu Wu), and NCEP/NCO (Dr. John Ward and his colleagues). We thank Don Johnson for fruitful discussions. Special thanks for evaluation and ongoing discussions are given to NCEP's Storm Prediction Center and Aviation Weather Center, to many NWS Regions and Forecast Offices, and to many others from the government and private sector who have noted issues and written us directly or through the RUC web forum (under the RUC web page at *http://ruc.fsl.noaa.gov*).

References

Benjamin, S.G., 1989: An isentropic mesoα-scale analysis system and its sensitivity to aircraft and surface observations. *Mon. Wea. Rev*., **117**, 1586-1603.

Benjamin, S.G., K. A. Brewster, R. L. Brummer, B. F. Jewett, T. W. Schlatter, T. L. Smith, and P. A. Stamus, 1991: An isentropic three-hourly data assimilation system using ACARS aircraft observations. *Mon. Wea. Rev*., **119**, 888-906.

Benjamin, S.G., K.J. Brundage, P.A. Miller, T.L. Smith, G.A. Grell, D. Kim, J.M Brown, and T.W. Schlatter, 1994: The Rapid Update Cycle at NMC. Preprints, *10th Conference on Numerical Weather Prediction*, AMS, Portland, OR, 566-568.

Benjamin, S.G., J.M. Brown, K.J. Brundage, D. Devenyi, G.A. Grell, D. Kim, B.E. Schwartz, T.G. Smirnova, T.L. Smith, S. S.Weygandt, and G.S. Manikin, 2002: RUC20 - The 20-km version of the Rapid Update Cycle. *NWS Technical Procedures Bulletin No. 490*. [FSL revised version available through RUC web site at http://ruc.fsl.noaa.gov]

Benjamin, S.G., G.A. Grell, J.M. Brown, T.G. Smirnova, and R. Bleck, 2004a: Mesoscale weather prediction with the RUC hybrid isentropic-terrain-following coordinate model. *Mon. Wea. Rev*., **132**, 473-494.

Benjamin, S.G., D. Dévényi, S.S. Weygandt, K.J. Brundage, J.M. Brown, G.A. Grell, D. Kim, B.E. Schwartz, T.G. Smirnova, T.L. Smith, and G.S. Manikin, 2004b: An hourly assimilation/forecast cycle: The RUC. *Mon. Wea. Rev*., **132**, 495-518.

Bleck, R., 1978: On the use of hybrid vertical coordinates in numerical weather prediction models. *Mon. Wea. Rev.,* **115**, 3097-3114.

Bleck, R., and D. Boudra, 1981: Initial testing of a numerical ocean model using a hybrid (quasi-isopycnic) vertical coordinate. *J. Phys. Oceanogr*., **11**, 755-770.

Bleck, R., and S.G. Benjamin, 1993: Regional weather prediction with a model combining terrain-following and isentropic coordinates. Part I: Model description. *Mon. Wea. Rev.,* **121**, 1770-1785.

Bleck, R., 2002: An oceanic general circulation model framed in hybrid isopycnic-Cartesian coordinates. *Ocean Mod*., **4**, 55-88.

Burk, S.D., and W.T. Thompson, 1989: A vertically nested regional numerical prediction model with second-order closure physics. *Mon. Wea. Rev*., **117**, 2305-2324.

Daley, R., 1991: *Atmospheric Data Analysis*. Cambridge University Press, Cambridge, 457 pp.

Davies, H. C., and R.E. Turner, 1977: Updating prediction models by dynamical relaxation: An examination of the technique. *Quart. J. Royal Meteor. Soc*., **103**, 225-245.

Deaven, D.G., 1976: A solution for boundary problems in isentropic coordinate models. *J. Atmos. Sci*., **33**, 1702-1713.

Devenyi, D., and S.G. Benjamin, 2003: A variational assimilation technique in a hybrid isentropic-sigma coordinate. *Meteor. Atmos. Phys.,* **82,** 245-257.

Drijfhout, S.Y., 1992: Ring genesis and the related heat transport. Part II: A model comparison. *J. Phys. Oceanog*., **22**, 268-285.

Dudhia, J., 1989: Numerical study of convection observed during the winter monsoon experiment using a mesoscale two-dimensional model. *J. Atmos. Sci*., **46**, 3077-3107.

Dutton, J.A., 1976*: The Ceaseless Wind*. McGraw-Hill, Inc., 579 pp.

Egger, J., 1999: Numerical generation of entropies. *Mon. Wea. Rev*., **127**, 2211-2216.

Eliassen, A., and E. Raustein, 1968: A numerical integration experiment with a model atmosphere based on isentropic coordinates. *Meteor. Ann.*, **5**, 45-63.

Gall, R., 1972: *Prediction of a quasi-steady jet core with an isentropic numerical model*. Ph.D. thesis, University of Wisconsin, 121 pp. [Available from The Schwerdtfeger Library, Space Science and Engineering Center, 1225 W. Dayton St., University of Wisconsin-Madison, Madison, WI 53706]

Gall R., and M.A. Shapiro, 2000: The influence of Carl-Gustav Rossby on mesoscale weather prediction and an outlook for the future. *Bull. Amer. Meteor. Soc.*, **81**, 1507-1523.

Grell, G.A., and D. Devenyi, 2002: A generalized approach to parameterizing convection combining ensemble and data assimilation techniques. *Geophys. Res. Lett.*, **29**, 38-1-4.

Gutman, S.I., and S.G. Benjamin, 2001: The role of ground-based GPS meteorological observations in numerical weather prediction. *GPS Solutions*, **4**, 16-24.

He, Z., 2002: A non-hydrostatic model with a generalized vertical coordinate. Ph.D. thesis, University of Miami, Coral Gables, FL, 99 pp.

Hirt, C.W., A.A. Amsden, and J.L. Cook, 1974: An arbitrary Langrangian-Eulerian computing method for all flow speeds. J. Comput. Phys., 14, 227--253.

Huang, X.-Y., and P. Lynch, 1993: Diabatic digital-filtering initialization: Application to the HIRLAM model. *Mon. Wea. Rev.*, **121**, 589-603.

Johnson, D.R., T.H. Zapotocny, F.M. Reames, B.J. Wolf, and R.B. Pierce, 1993: A comparison of simulated precipitation by hybrid isentropic-sigma and sigma models. *Mon. Wea. Rev.,* **121**, 2088-2114.

Johnson, D.R., 1997: "General coldness of climate models" and the second law: Implications for modeling and earth system. *J. Climate*, **10**, 2826-2846.

Johnson, D.R., and Z. Yuan, 1998: The development and initial tests of an atmospheric model based on a vertical coordinate with a smooth transition from terrain following to isentropic coordinates. *Advances in Atmos. Sciences*, Vol., 15, No. 3, 283-299.

Johnson, D.R., A.J. Lenzen, T.H. Zapotocny, and T.K. Schaack, 2000: Numerical uncertainties in the simulation of reversible isentropic processes and entropy conservation. *J. Climate,* **13**, 3860-3884.

Johnson, D.R., A.J. Lenzen, T.H. Zapotocny, and T.K. Schaack, 2002: Numerical uncertainties in simulation of reversible isentropic processes and entropy conservation: Part II. *J. Climate*, **15**, 1777-1804.

Kim, D., S.G. Benjamin and J.M. Brown, 2002: Cloud/hydrometeor initialization in the 20-km RUC using radar and GOES data. Preprints, *15th Conf. Num. Wea. Pred.*, San Antonio, TX, Amer. Meteor. Soc., 335-338.

Konor, C.S., and A. Arakawa, 1997: Design of an atmospheric model based on a generalized vertical coordinate. *Mon. Wea. Rev.,* **125**, 1649-1673.

Moninger, W.R., R.D. Mamrosh, P.M. Pauley, 2003: Automated meteorological reports from commercial aircraft. *Bull. Amer. Meteor. Soc.*, **84**, 203-216.

Pan, Z.-T., S.G. Benjamin, J.M. Brown, and T.G. Smirnova, 1994: Comparative experiments with MAPS on different parameterization schemes for surface moisture flux and boundary-layer processes. *Mon. Wea. Rev.,* **122**, 449-470.

Phillips, N.A., 1957: A coordinate system having some special advantages for numerical forecasting. *J. Meteor*., **14**, 184-185.

Purser, R.J., S.K. Kar, S. Gopalakrishnan, S., 2002: A semi-lagrangian non-hydrostatic model employing a hybrid vertical coordinate. Preprints, *15th Conf. on Num. Wea. Pred.*, Amer. Meteor. Soc., San Antonio, 248-251.

Reisner, J., R.M. Rasmussen, and R.T. Bruintjes, 1998: Explicit forecasting of supercooled liquid water in winter storms using the MM5 mesoscale model. *Quart. J. Roy. Meteor. Soc.*, **142**, 1071-1107.

Riishojgaard, L. P., 1998: A direct way of specifying flow-dependent background error correlations for meteorological analysis systems. *Tellus*, **50A**, 42-57.

Rogers, E., D. Parrish, and G. DiMego, 1999: Changes to the NCEP operational Eta model. NOAA/NWS Technical Procedures Bulletin No. 454. [Available from National Weather Service, Office of Climate, Water, and Weather Services, 1325 East-West Highway, Silver Spring, MD 20910, also available at http://www.nws.noaa.gov/om/tpbpr.shtml]

Rossby, C.-G., and collaborators, 1937: Isentropic analysis. *Bull. Amer. Meteor. Soc.*, **18**, 201-209.

Schreiner, A.J., T.J. Schmit, W.P. Menzel, 2001: Clouds based on GOES sounder data. *J. Geophys. Res.*, **106** (D17), 20349-20363.

Smirnova, T.G., J.M. Brown, and S.G. Benjamin, 1997: Performance of different soil model configurations in simulating ground surface temperature and surface fluxes. *Mon. Wea. Rev.*, **125**, 1870-1884.

Smirnova, T.G., J.M. Brown, S.G. Benjamin, and D. Kim, 2000a: Parameterization of cold season processes in the MAPS land-surface scheme. *J. Geoph. Res,* **105** (D3), 4077-4086.

Smirnova, T.G., S.G. Benjamin, J.M. Brown, B. Schwartz, and D. Kim, 2000b: Validation of long-term precipitation and evolved soil moisture and temperature fields in MAPS. Preprints, *15th Conf. on Hydrology,* Amer. Meteor. Soc., Long Beach, CA, 43-46.

Skamarock, W.C., 1998: A hybrid-coordinate nonhydrostatic atmospheric model. *12th Conf. on Num. Wea. Pred.*, AMS, Phoenix, 232-235.

Thompson, G., R.M. Rasmussen, and K. Manning, 2004: Explicit forecasts of winter precipitation using an improved bulk microphysics scheme. Part I: description and sensitivity analysis. *Mon. Wea. Rev.*, **132**, 519-542.

Uccellini, L.W., D.R. Johnson, and R.E. Schlesinger, 1979: An isentropic and sigma coordinate hybrid numerical model: Model development and some initial tests. *J. Atmos. Sci.*, **36**, 390-414.

Weaver, C.J., A.R. Douglass, and R.B. Rood, 2000: Lamination frequencies as a diagnostic for horizontal mixing in a 3D transport model. *J. Atmos. Sci.*, **57**, 247-261.

Wolfe, D.E. and S.I. Gutman, 2000: Development of the NOAA/ERL ground-based GPS water vapor demonstration network: Design and initial results. *J. Atmos. Ocean. Tech.*, **17**, 426-440.

Zapotocny, T.H., D.R. Johnson, and F.R. Reames, 1994: Development and initial test of the University of Wisconsin global isentropic-sigma model. *Mon. Wea. Rev.*, **122**, 2160-2178.

Zhu, Z., J. Thuburn, and B.J. Hoskins, 1992: A vertical finite-difference scheme based on a hybrid σ-θ-p coordinate. *Mon. Wea. Rev.*, **120**, 851-862.

Zhu, Z., and E.K. Schneider, 1997: Improvement in stratosphere simulation with a hybrid σ-θ coordinate GCM. *Quart. J. Royal Meteor. Soc.,* **123**, 2095-2113.

Model/assimilation system	**Horizontal resolution**	**Number of vertical levels**	**Assimilation frequency**	**Implemented at NCEP**
RUC1	60 km	25	3 h	September 1994
RUC2	40 km	40	1 h	April 1998
RUC20	20 km	50	1 h	April 2002

Table 1. A history of spatial resolution and assimilation frequency in implementations of the operational Rapid Update Cycle at NCEP.

level	**1**	**2**	**3**	**4**	**5**	**6**	**7**	**8**	**9**	**10**
θ_v	224	232	240	245	250	255	260	265	270	273
level	**11**	**12**	**13**	**14**	**15**	**16**	**17**	**18**	**19**	**20**
θ_v	276	279	282	285	288	291	294	296	298	300
level	**21**	**22**	**23**	**24**	**25**	**26**	**27**	**28**	**29**	**30**
θ_v	302	304	306	308	310	312	314	316	318	320
level	**31**	**32**	**33**	**34**	**35**	**36**	**37**	**38**	**39**	**40**
θ_v	322	325	328	331	334	337	340	343	346	349
level	**41**	**42**	**43**	**44**	**45**	**46**	**47**	**48**	**49**	**50**
θ_v	352	355	359	365	372	385	400	422	450	500

Table 2. Target θ_v values (K) for the RUC20 (50 levels).

	σ - pressure	θ-σ generalized
Predefined	$\sigma_p(k)$	Δp_{min}
	p_{top}	$\theta_{v-ref}(k)$
Adaptively based on		
	p_{sfc}	p_{sfc}
		θ_v

Table 3. Definition of 3-D pressure field contrasted in σ - pressure vs. θ-σ generalized vertical coordinates. Variables for which predefined values must be set are shown for each coordinate system, as well as the variables used in the adaptive definition of the 3-d pressure field.

Data Type	~Number	Frequency
Rawinsonde (including special obs)	80	/12 h
NOAA 405 MHz profiler wind	31	/ 1 h
Boundary-layer (915 MHz) profiler wind	24	/ 1 h
RASS virtual temperatures	10	/ 1 h
VAD winds (WSR-88D radars)	110-130	/ 1 h
Aircraft (ACARS) (wind, temperature)	1400-4500	/ 1 h
Surface/METAR − land (V, p_{sfc}, T, T_d)	1500-1700	/ 1 h
Surface/Mesonet – land	2500-4000	/ 1 h
Buoy	100-150	/ 1 h
GOES precipitable water	1500-3000	/ 1 h
GOES cloud drift winds	1000-2500	/ 1 h
GOES cloud-top pressure/temp	~10 km res	/ 1 h
SSM/I precipitable water	1000-4000	/ 6 h
GPS precipitable water	165	/ 1 h
Ship reports	10s	/ 3 h
Reconnaissance dropwinsonde	0 - a few	/ variable

Table 4. Observational data used in the RUC as of spring 2003.

Variables in native RUC analysis analysis		**Updating from observations in RUC**
p	pressure	MV analysis from z increment, hybrid adjust
θ_v	virtual potential temperature	MV analysis, UV θ_v analysis
u,v	horizontal wind components	MV analysis
q_v	water vapor mixing ratio	Moisture analysis outer loop
q*	hydrometeor mixing ratios (cloud water, ice, rain water, snow, graupel) and ice particle number concentration	Cloud analysis with GOES cloud-top data
land-surface variables		
	soil temperature, snow temp – top level	From MV and UV θ_v analysis increment at lowest atmospheric level
	soil moisture	Not modified
	snow water equivalent	Not modified
(z calculated hydrostatically, all p/z obs converted to z innovations at a given pressure)		

Table 5. RUC native coordinate variables and modification in the RUC analysis. MV refers to multivariate mass/wind analysis and UV to univariate analyses.

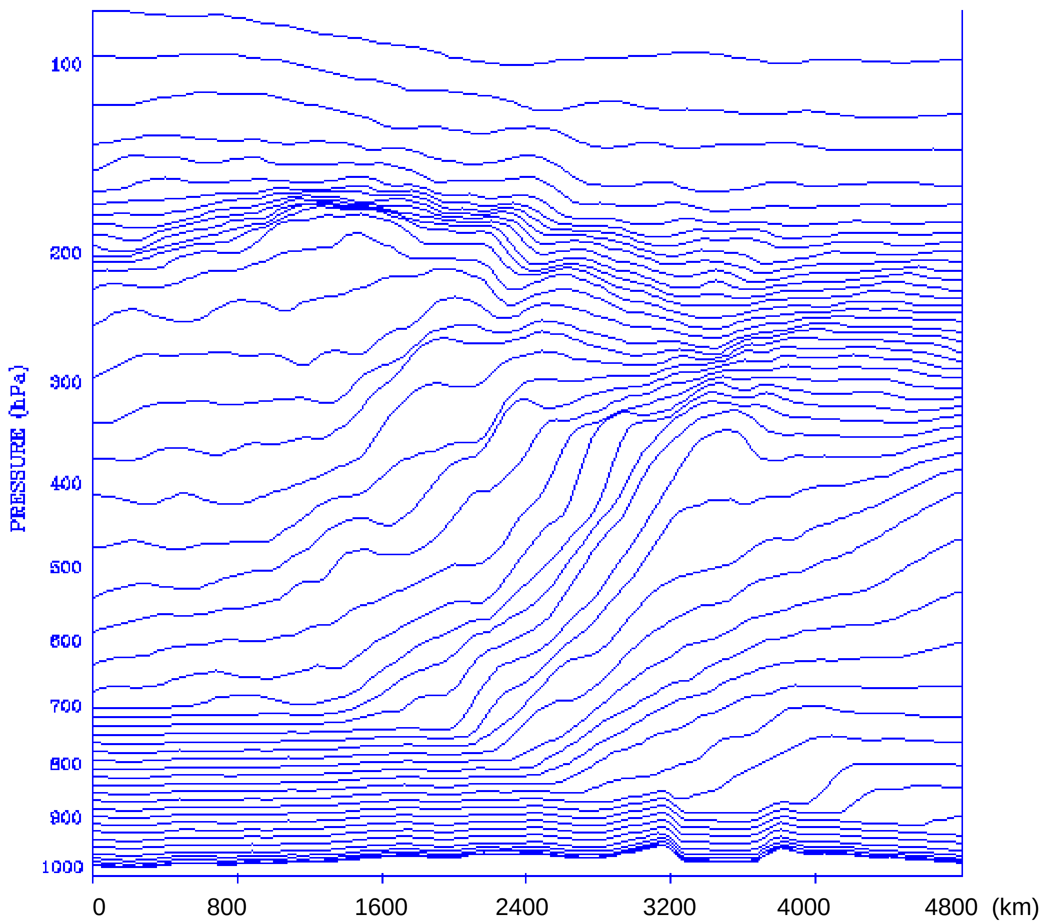

Fig. 1. Vertical cross section showing RUC native coordinate (isentropic-sigma hybrid) levels for 20-km RUC with 50 levels. Data are taken from a RUC 12-h forecast valid at 1200 UTC 2 April 2002. Cross sections are oriented from south (Mississippi) on left to north (western Ontario) on right.

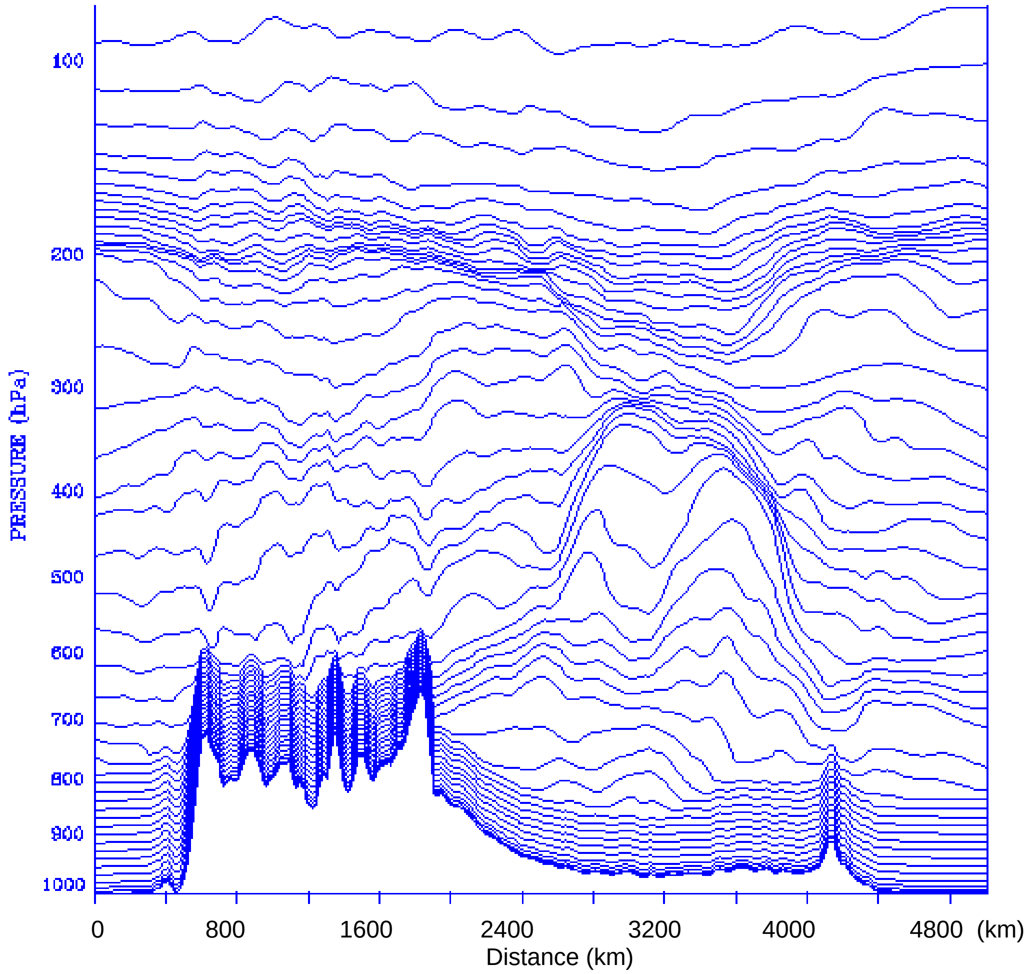

Fig. 2. Vertical cross section of RUC hybrid isentropic-sigma coordinate levels for 1800 UTC 14 January 2002. Cross-section orientation is approximately west-east through California (left), Colorado (center), and the Appalachian Mountains (right).

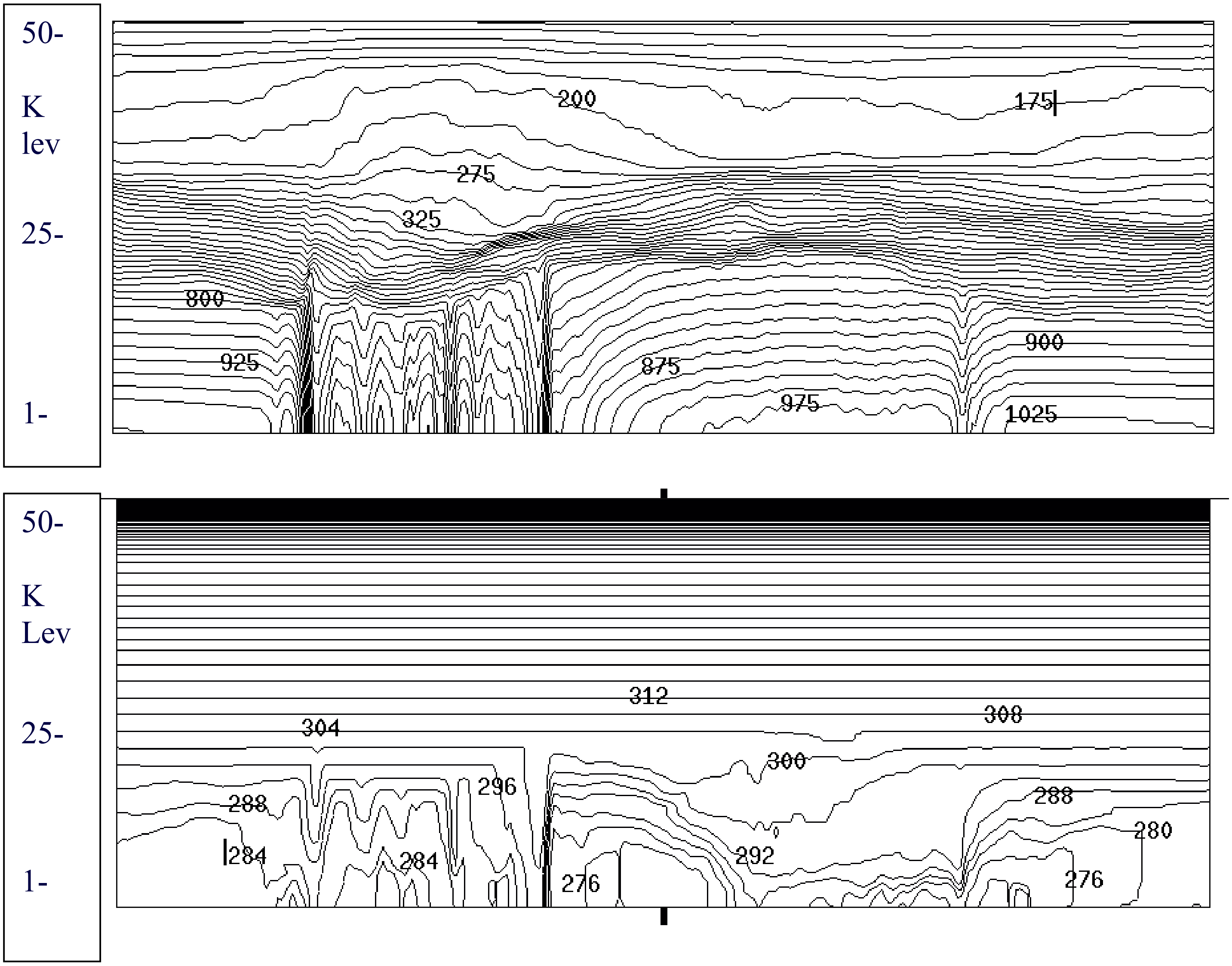

Fig. 3. Vertical cross sections of RUC native coordinate levels with vertical axis as vertical native k level (1-50), for same winter case as shown in Fig. 2. a) Pressure (contour interval 25 hPa), b) virtual potential temperature (contour interval 4 K).

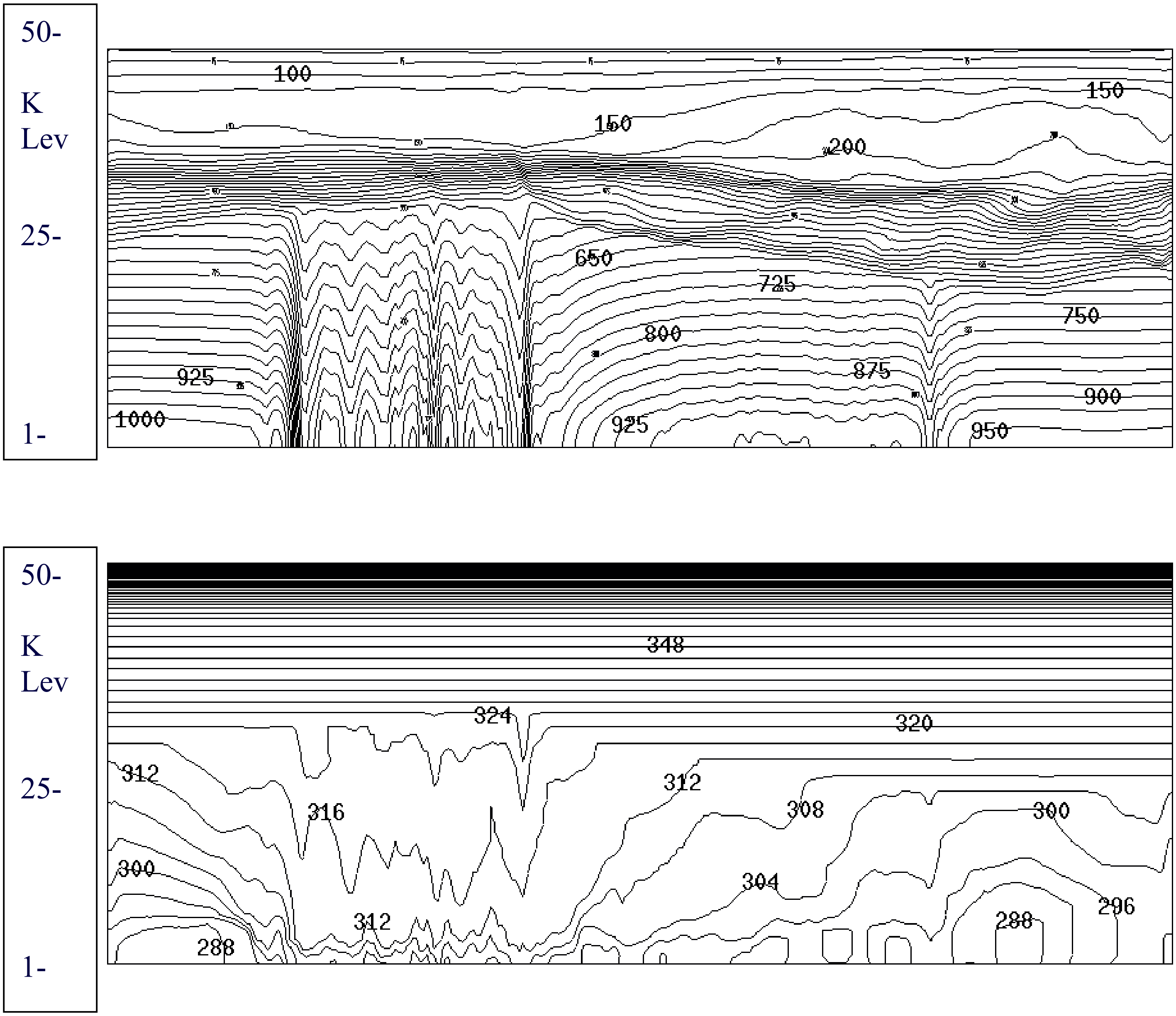

Fig. 4. Same as Fig. 3, except for a summer case (25 July 2001 1800 UTC) instead of a winter case. Horizontal location is same as in Figs. 2 and 3, west-east across the RUC domain, through California, Colorado, and Virginia.

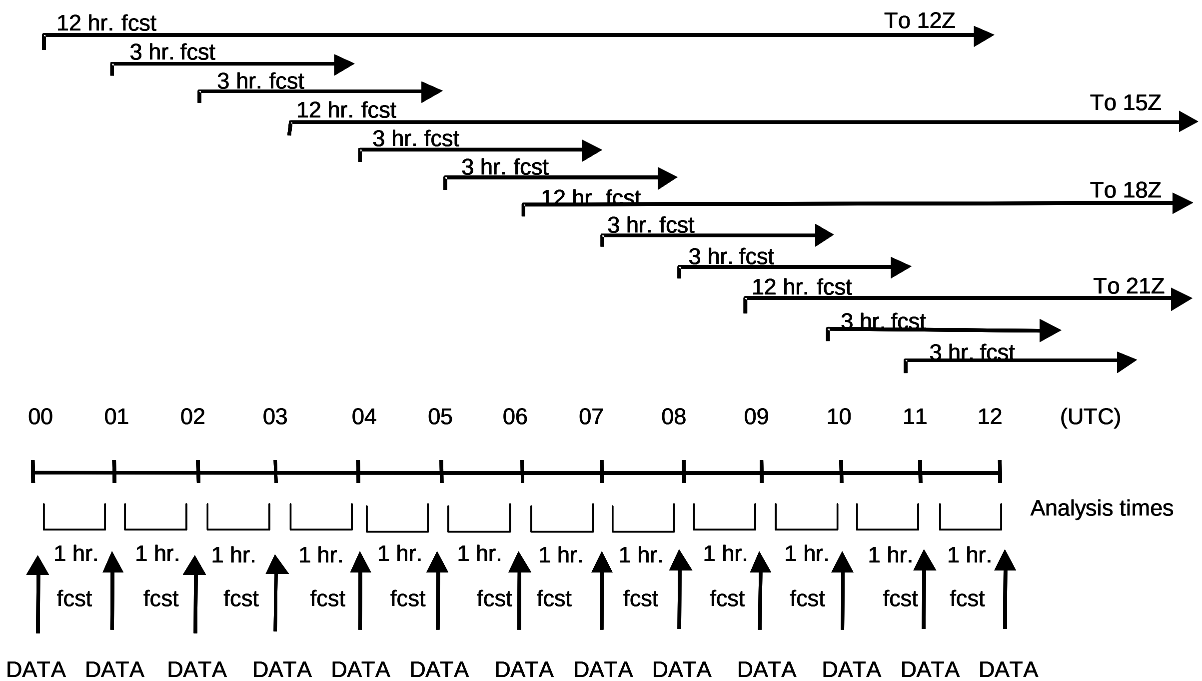

Fig. 5. Schematic of 1-h Rapid Update Cycle operational configuration over a 12-h period. As at NCEP in early 2003.

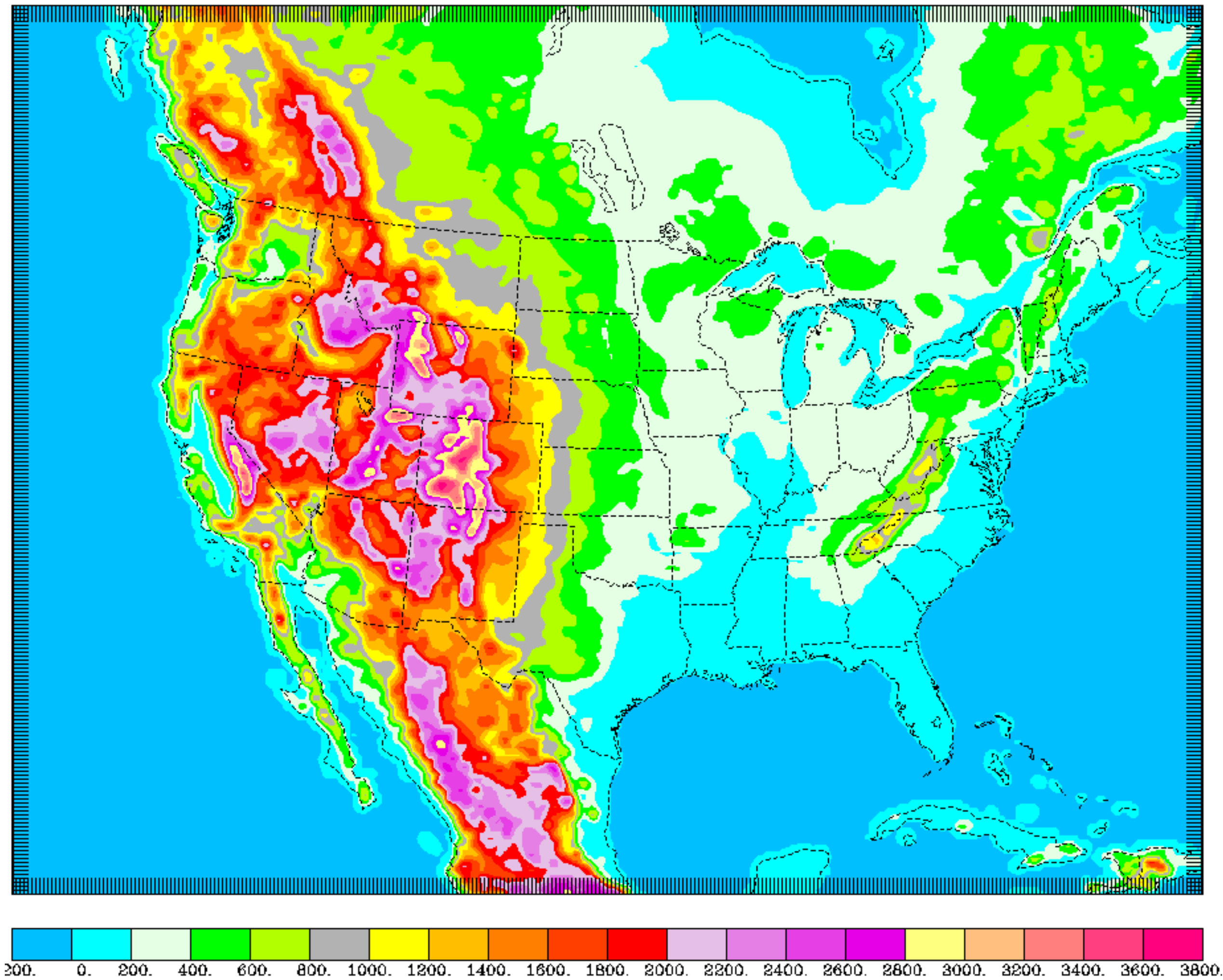

Fig. 6. Domain and terrain elevation of the 20-km version of the RUC. Contour elevation is 200 m. Grid dimensions are 301 by 225 points.

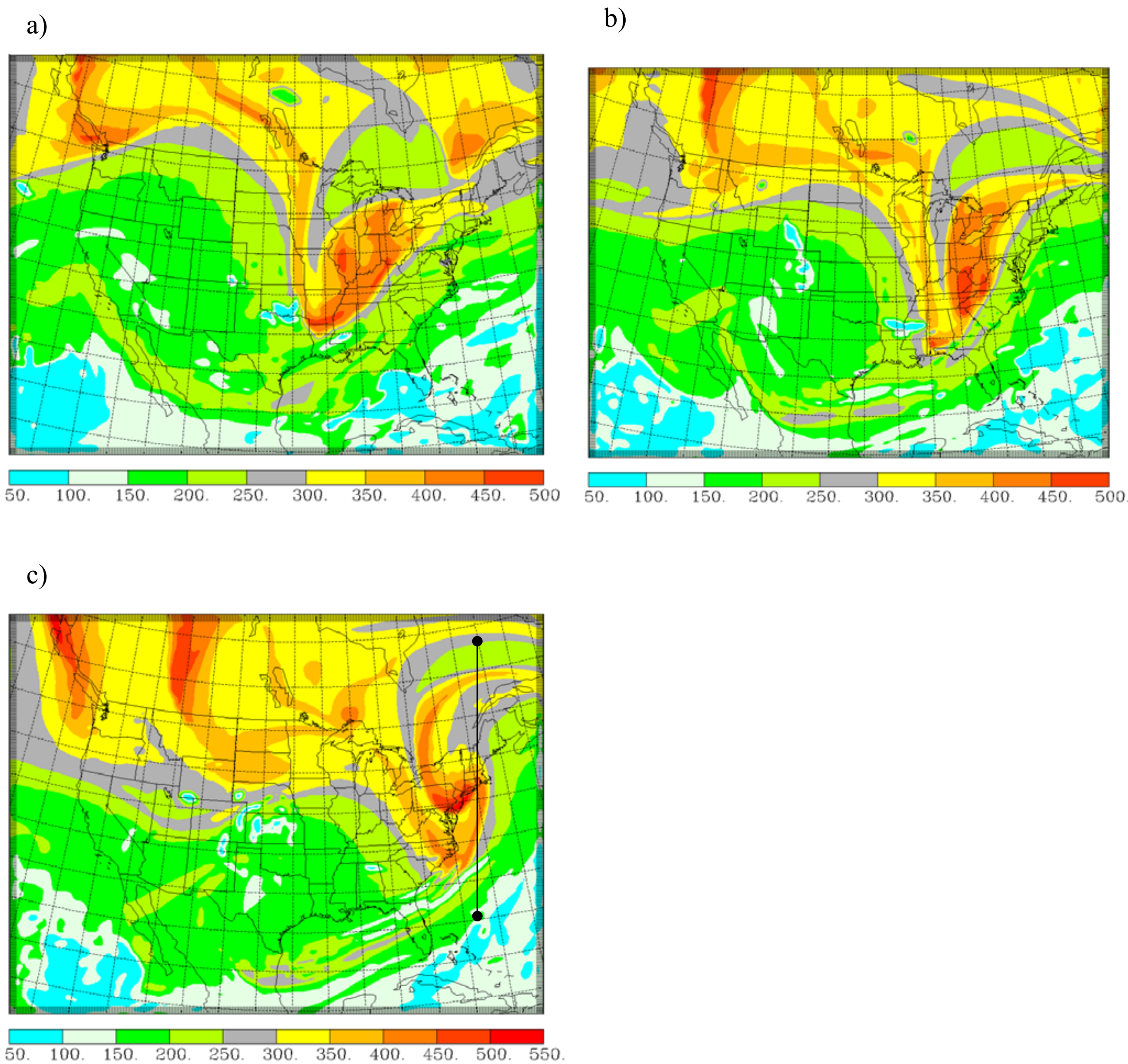

Fig. 7. Pressure (hPa) of the dynamic tropopause (defined in text) from 20-km RUC forecast initialized at 1200 UTC 4 February 2001. a) 12-h forecast, b) 24-h forecast, c) 36-h forecast. Line through eastern part of domain is location of vertical cross sections shown in Fig. 8.

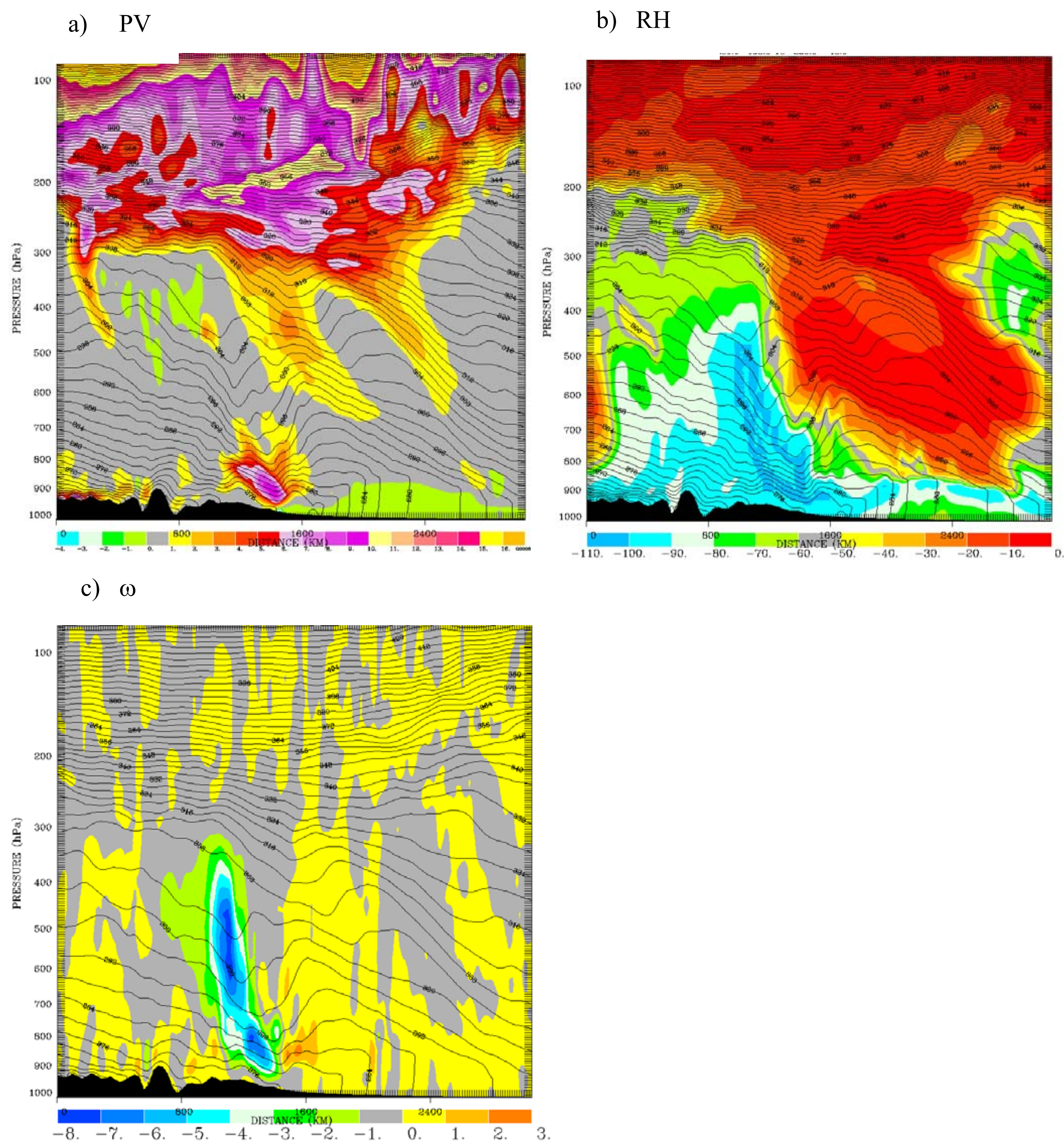

Fig. 8. Vertical cross sections from 36-h forecasts from 20-km RUC model along north-south line shown in Fig. 7c for potential temperature (solid lines, every 4 K) and a) potential vorticity (PVU), b) relative humidity (%), and c) vertical velocity ($\times$ 10 μb s^{-1}; -7 = -70 μb s^{-1}).